Sumatra Earthquake Dynamics and Expanding Earth theory

Abstract

Seismic tomographies under the Sunda Arc, retraced at the same horizontal and vertical scale. a) S-wave tomography by Ritzwoller *et al.* (2005) along the line A-A' (see insert for location of the profile) has been redrawn. The resolving power has produced a tomographic image up to the depth of 250 km. The earthquakes of the Wadati-Benioff zone also do not exceed 250 km in depth. A wedge-shaped high velocity zone (blue zone) extending deeper than 100 km is revealed. b) P-wave tomography by Hafkenscheid *et al.* (2001) along the section B-B' (see insert) has been redrawn. This technique allows a deeper testing of the mantle elastic properties. The wedge of anomalous high velocity mantle can be traced up to a depth of more than 1000 km. The wedge appears more defined and more vertical in the P-tomography. In this paper an idea is proposed – on the basis of several lines of evidence – that the Great Sumatra earthquake was caused by upward movements of this mantle wedge.

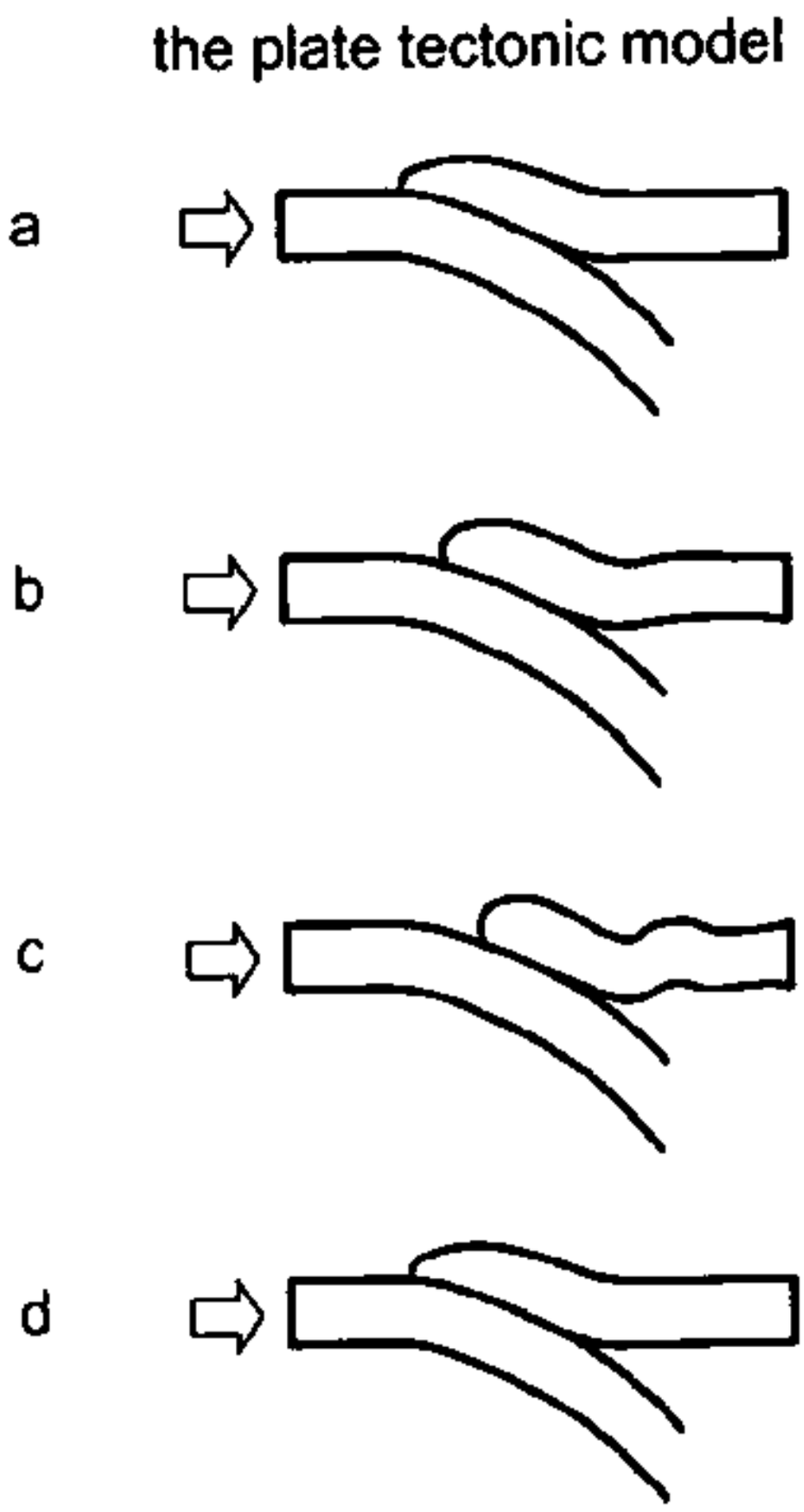

Fig. 4. The elastic model for the occurrence of the shallow earthquakes caused by subduction. The mechanism of accumulation and release of potential energy is considered to be purely elastic in a brittle environment, and is called the elastic rebound model. The Sumatra earthquake was a shallow event, so this model can be adopted. a) Plunging lithosphere moves – at a rate of a few centimetres per year – from the surface toward the transition zone and further on. b) Friction and asperities stick the backarc lithosphere to the plunging oceanic lithosphere allowing them to travel fastened together. c) Fracture starts in the Wadati-Benioff zone allowing the backarc lithosphere to rebound elastically toward the surface, and the subducting lithosphere – free of braking – to suddenly accelerate. d) Two lithospheric slabs have completed their rebound and are ready in case for a new cycle. It should be noted that the commonly accepted fault plane solution of the Sumatra earthquake assumes a nearly horizontal slip surface; its horizontality making the above drawn model very difficult to work.

subvertical fracture (Figure 6c) is produced by a sudden uplift of subcrustal or sublithospheric material being pushed upward by a phase change triggered by the tensional regime. The uplifted face may have a downward rebound, which would produce a tilt of the neighbouring plate (Figure 6c). This is consistent with the observed uplift of the coralline barrier to the west and the subsidence of the larger islands. Finally, a large number of aftershocks would be produced on new faults (Figure 6d) and along the entire major fault, in a wide area. Lateral spreading of the arc could also be triggered by the main rupture (Figure 6d).

This model should lead to a longer fault length. This confirmed by an elongated as the P1 solution. This is because an elongated distribution of epicentres of aftershocks Mw ≥ 6.0 occurred within two hours and within two days after the main shock (see in Table 1 the very preliminary epicentres of 26 and 27 December 2004; see also the map in Figure 7) — an elongation of ≈1200 km.

If the P1 horizontal solution were the fault plane we would expect an immediate activation of the entire alleged fault surface (rectangular boundary in Figure 7). However, this fault surface has apparently not shown the expected immediate high-magnitude aftershock activity. This might represent an important clue favouring a vertical fault solution such as P2, extending more than 1200 km from west Sumatra to the northern tip of the Andaman Islands (see the bold dotted line in Figure 7). The expected series of aftershocks occurred in this long region. It should be noted that the first large aftershock (M_w=6.2; T=1:21:18; Lat=6.37; Lon=93.36) was more than 3° north of the epicentre of the main shock. The second major aftershock (M_w=6.0; T=2:51:59; Lat=12.49;

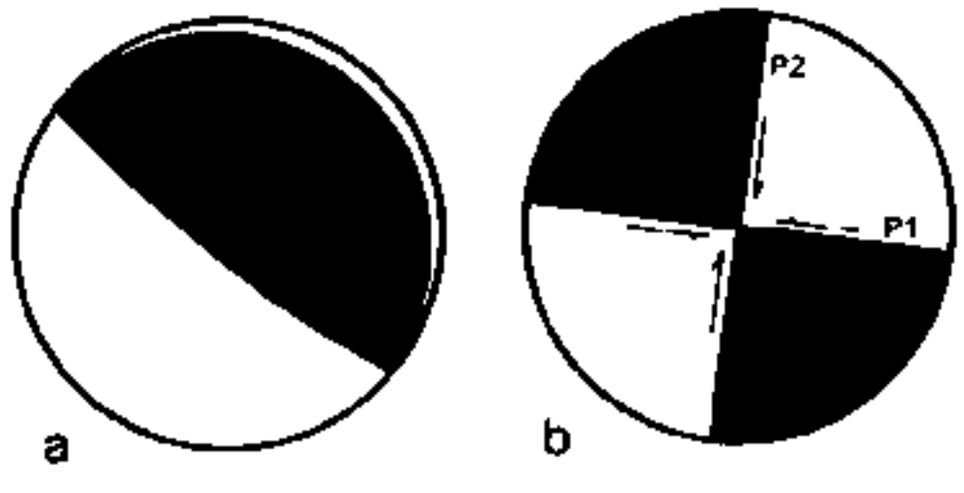

Fig. 5. Focal mechanism. a) Centroid moment tensor (CMT) solution of Harvard is reproduced. Indeed, the CMT provides two possible fault plane solutions for the Sumatra earthquake: P1: (Strike=329; Dip=8; Slip=110) and P2: (Strike=129; Dip=83; Slip= 87). The solution P1 is commonly adopted because of compatibility with the plate tectonic model. b) Section of the focal sphere on a vertical plane perpendicular to the strike direction, and the two conjugate fault planes labelled P1 and P2. The P1's very low dip angle of 8° has led to assumption of a sub-horizontal slip. However, many clues are in favour of the nearly vertical fault solution P2.

Table 1

M	Day	Time	Lat	Lon	Depth	
9.0	26/12/2004	0:58:50	3.244	95.825	10	off the west coast of northern Sumatra
6.2	26/12/2004	1:21:18	6.372	93.363	10	Nicobar islands, India region
6.0	26/12/2004	2:51:59	12.494	92.582	10	Andaman islands, India region
7.5	26/12/2004	4:21:25	6.891	92.891	10	Nicobar islands, India region
6.5	26/12/2004	9:20:01	8.867	92.382	10	Nicobar islands, India region
6.2	26/12/2004	10:19:30	13.455	92.791	10	Andaman islands, India region
6.3	26/12/2004	11:05:01	13.542	92.877	10	Andaman islands, India region
6.2	26/12/2004	19:19:53	2.770	94.158	10	off the west coast of northern Sumatra
6.0	27/12/2004	0:32:13	5.502	94.465	10	northern Sumatra, Indonesia
6.1	27/12/2004	0:49:27	12.978	92.449	10	Andaman islands, India region
6.1	27/12/2004	9:39:03	5.379	94.706	10	northern Sumatra, Indonesia
6.0	27/12/2004	10:05:00	4.762	95.111	10	northern Sumatra, Indonesia

(USGS preliminary data; released on Dec. 29, 2004)

Lon=92.58) was more than 9° north of the main event. These events occurred less than 2 hours apart. The elongated space window and the narrow time window strongly suggest that these events were true aftershocks on the same long structure. The non perfect plain-shape of the rupture surface is not a problem for a vertical fracture (also zigzag fracture could be allowed) while grater mechanical problems arises for a >1000 km length subhorizontal fault in developing along such long arched thrust front.

The elongated shape of the fault also agrees with a quick calculation of the length of the high frequency P-wave record on seismograms (Lomax, 2005; Lomax and Michelini, 2005). The P-wave radiation was compatible in duration with a fault rupture propagation of at least 1100 km. The NNW directivity of initial propagation is assured by the characteristic different length and frequency – Doppler effect – of the P wave train recorded at different azimuths (Bilham, 2005a; Ishii *et al.*, 2005).

It is true that the inconsistency of the plate tectonics bias in adopting the P1 fault-plane solution was not recognized in papers devoted to the great Sumatra earthquake. However, the need for a steeper slip plane was mentioned in a normal-mode analysis by Park *et al.* (2005).

THE USGS PRELIMINARY HYPOCENTRAL DATA AND THE HARVARD CMT CATALOGUE

I have extracted seismic data from the USGS global catalogue with the further aim of analyzing the 3-D distribution of preliminary hypocenters. The data were partitioned in a two-hours time-window from the origin time of the main shock, then in two days window from the origin time and up to the end of February 2005. I consider especially the first two shorter time windows, as I believe that a seismic event (*sensu lato*) is better characterized by what happens immediately after the main shock.

The data from December 26, 00h 00m 00s, to December 27, 24h 00m 00s, are listed in Table 2, and the selected events are chronologically numbered. Events that have a CMT fault solution in the Harvard catalogue are shown with an asterisk. Double asterisks indicate the presence of CMT solutions plotted in Figure 9c.

All the extracted sets of data contain subsets of a large number of earthquakes whose depths were fixed at 30 km. Because of inadequate focal depth control, I removed them from the figures.

In Figure 8a a complete set of 20 events ($M \geq 5.5$) which occurred in the first two hours from the main event is shown as red circles. The projection of the hypocenters on the XZ plane (grey circle) shows more clearly the presence of events with fixed 30 km depths. These events are not just of unknown depth but due to computational effects the same uncertainty is reflected in latitude and longitude errors. The main shock (large red dot in Figure 8a) is a member of this subset. The same computational difficulty made it impossible to determine the focal mechanisms for nearly all aftershocks up to the evening of December 26. In Figure 8b the same time and magnitude window is shown without the 30km-depth data – but including the main shock. Then the total number is decreased to seven events.

The distribution of these hypocenters, numbered from 1 (main shock) to 7, is crustal and undercrustal, covering from

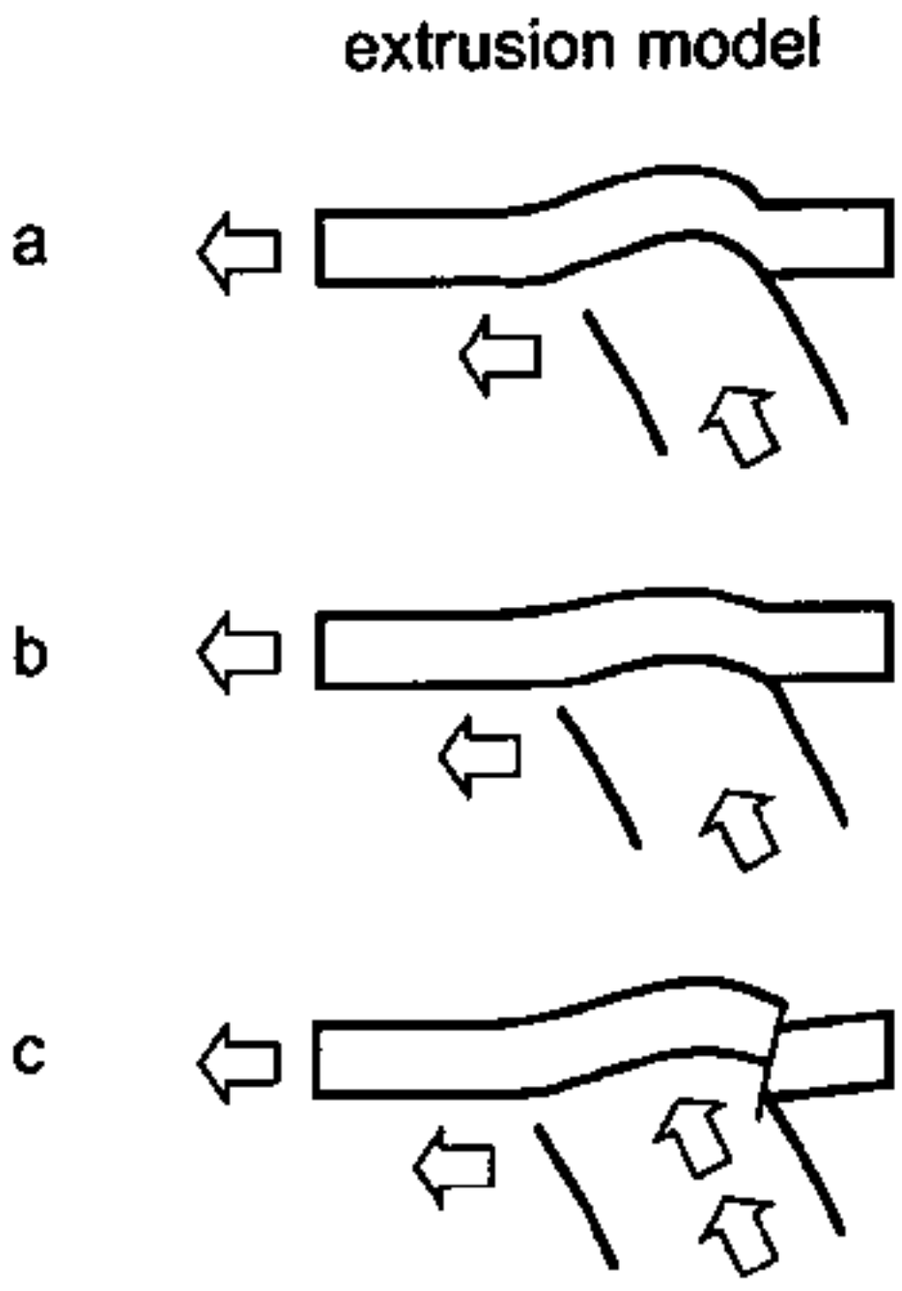

Fig. 6. Alternative model of the shallow arc-zone earthquake occurrence. a) Initially a process of decoupling of oceanic and continental lithosphere slowly occurs under the arc. b) The effect of this tensional regime is the subsidence of the bumping arc as witnessed by the coral reef subsidence. c) Nearly vertical fracture is eventually produced by a sudden uplift of undercrustal or underlithospheric material pushed upward by a sudden phase change triggered by the tensional regime. The lifted side can have, possibly, a downward rebound, producing a tilting of the neighbouring plate. This can be in agreement with the observed uplift of the coralline barrier to the west and the subsidence of the coasts to the east. d) Finally a plethora of settling new faulting, producing a high number of aftershocks, should be widely expected along the entire major fault in a wide area. Lateral spreading of the arc can also be triggered by the main fracture. This spreading can produce subhorizontal fault mechanisms.

a minimum depth of 15 km to a maximum depth of 51 km. The depth scale is exaggerated more than 10 times. While plate tectonics would expect a focal distribution dipping to the northeast, if we observe the seismicity from a high zenithal point displaced a little toward north (Figure 8c) it actually dips slightly to the southwest – consider the good alignment of the hypocenters 7, 5, 2, 3, and 1. The events do not occur on the alleged subduction interface.

I repeated the same system of plotting with a time window lasting for two days (26 and 27 December). In Figure 9a the total number of events, 56 hypocenters, is shown with their projection on the XZ plane. The 56 events are listed in Table 2. After elimination of the events with a pre-assigned depth of 30 km, the remaining 29 hypocenters are shown in Figure 9b and 9c. No well-defined NNE dipping subduction trend can be detected. In Figure 9a-c a small group of hypocenters at a depth of nearly 50 km is spotted near event number 3 in Figure 8b and c. In Figure 9d, in order to facilitate the understanding of the spatial-temporal pattern, chronological numbers are shown for the 29 selected events.

The focal mechanisms of aftershocks have been published after the second half of 26 December. Many of them are inconsistent with sub-horizontal subduction. Harvard CMT focal mechanisms are shown in Figure 9c and numbered following the event numbers of Figure 9d.

THE SEISMIC MOMENT

The definition of seismic moment is:

$$M_o = \mu \cdot s \cdot A \qquad (3)$$

with μ the shear modulus of the material, s the mutual dislocation of the two sides of the fault, and A the area of the fracture surface. The moment magnitude is defined in terms of the seismic moment:

$$M_w = \frac{2}{3}\log_{10} M_o - 10.7 . \qquad (4)$$

The longest-period normal modes of the earth, ${}_0S_2$ and ${}_0S_3$ were analyzed by Stein and Okal (2005). They yield a moment $M_o = 1.3 \cdot 10^{30}$ dyn·cm, three times larger than $M_o = 4.0 \cdot 10^{29}$ dyn·cm evaluated from long-period surface waves. From (4) an ultra-long period magnitude, $M_w = 9.3$, results, which is significantly larger than the previously reported $M_w = 9.0$.

The fact that the ultra-long period moment is higher than that from 300-s surface waves used by the Harvard CMT project reflects a significant physics process we may misunderstand. The interpretation of Stein and Okal (2005) is that a fast slip of several meters occurred on the southern third (around 400 km) of the sub-horizontal fault. Only this part of the total length of the fault would be responsible for the long-period surface wave excitation. A slower slip would have occurred on the northern two thirds of the fracture

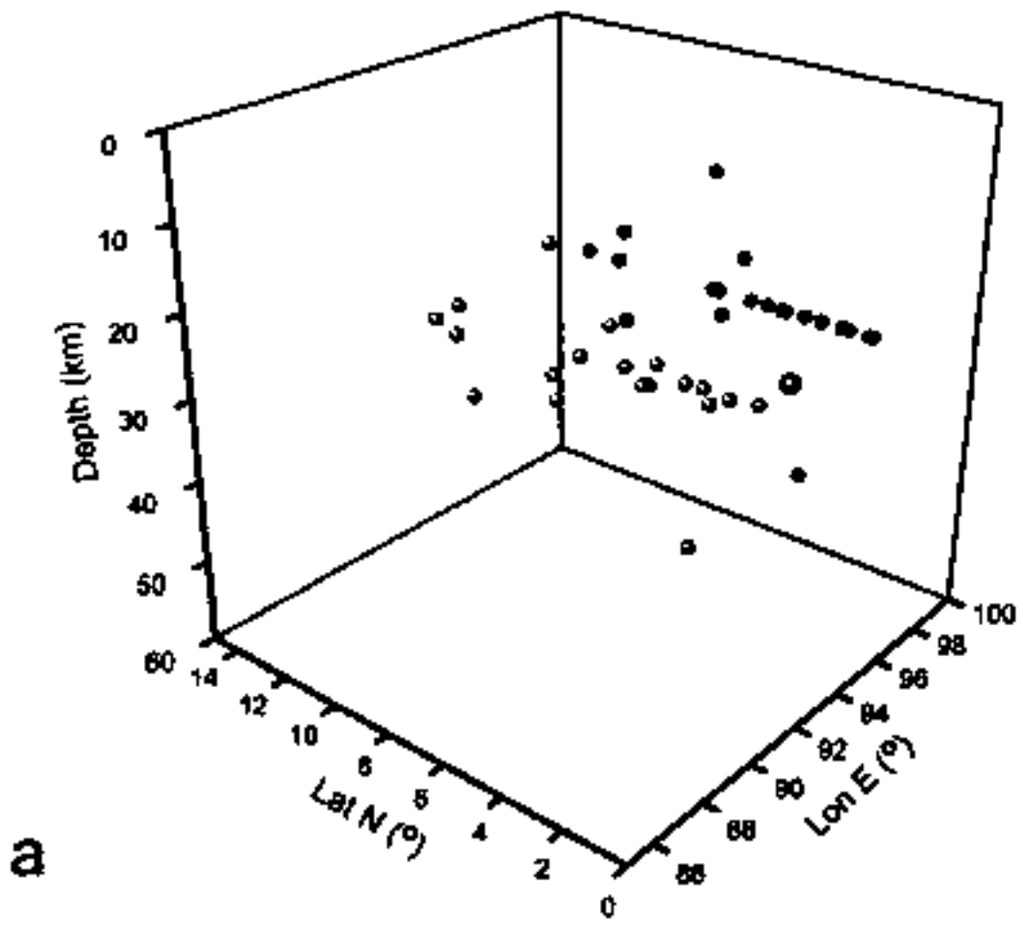

a

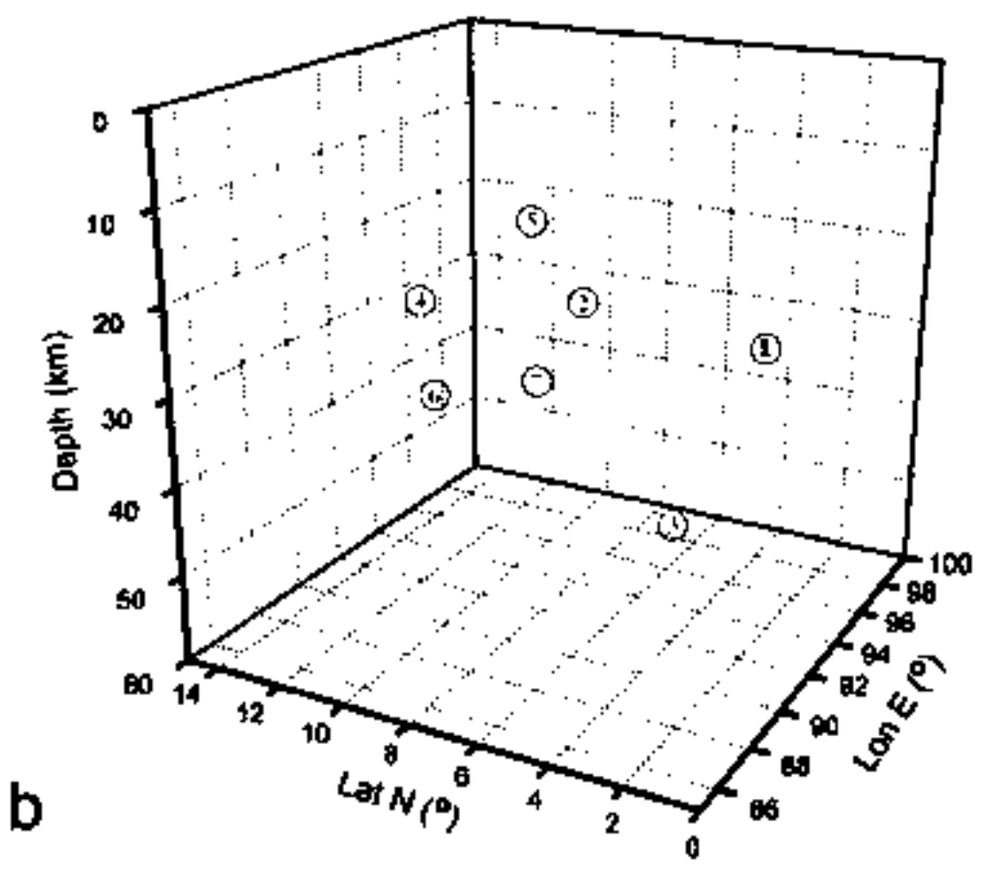

b

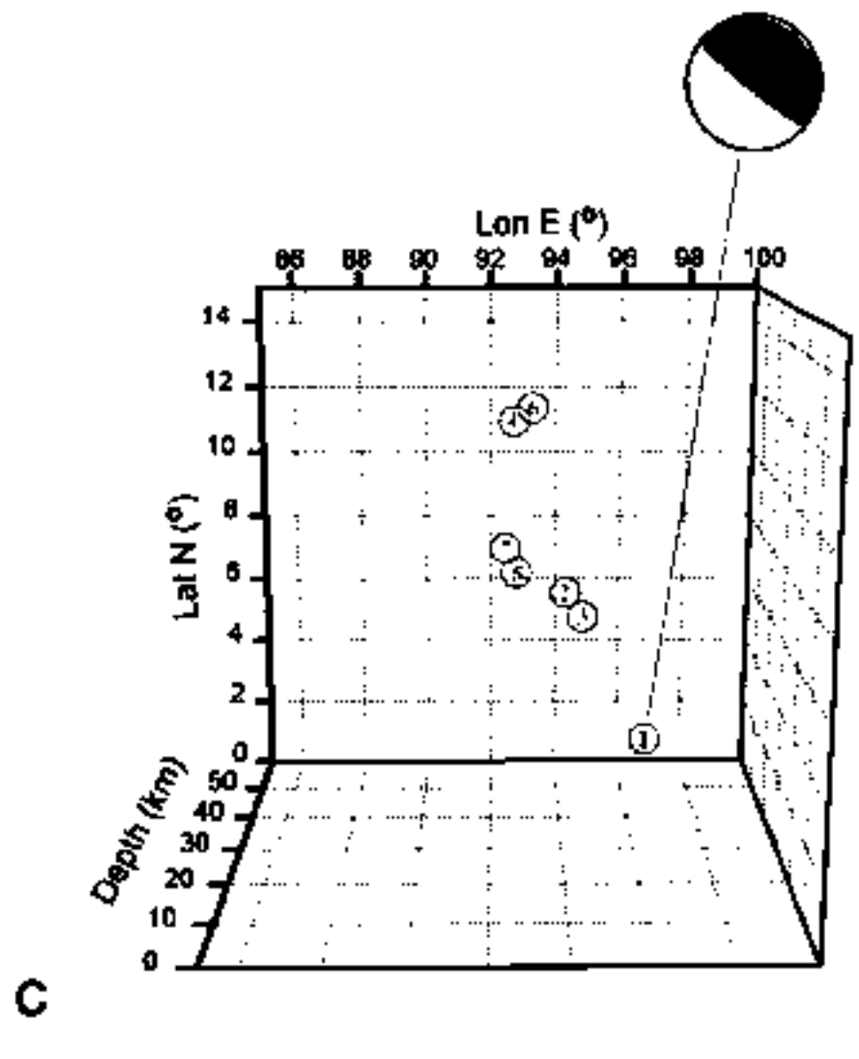

c

Fig. 8. a) A complete set of hypocenters (20 events; M ≥ 5.5) which occurred in the first two hours from the main event is shown in red spheres. If the hypocenters are projected on the XZ plane (grey circle), it becomes evident the existence of a number of depths fixed at 30 km. The events of this subset are of uncertain depth and also of large uncertainty in latitude and longitude epicentral coordinates. Also the main shock (greater sphere) is a member of this subset. b) The same time and magnitude window is shown after discarding the subset of the 30km-depth data – except the main shock. The total number–is decreased to 7 events. The distribution of the hypocenters – numbered chronologically from 1 (main shock) to 7– is crustal and undercrustal, covering from a minimum of 15 km to a maximum of 51 km. c) While the plate tectonics expects a distribution dipping northeastward, if we observe nearly vertically the distribution (Figure 8c), it can be seen that it dips slightly to the southwest, rather than along the alleged subduction slab. The vertical scale in a), b) and c) is exaggerated by more than 10 times, consequently great attention must be paid in judging the dipping angles.

which would have mostly excited the normal modes of the Earth. However, because the envisaged subhorizontal slip, this interpretation cannot account for the 10 cm displacement of the polhody path in a non-double-couple treatment. Indeed, horizontal displacements, referring to Figure 2, are in a plane perpendicular to the page and near parallel to the Earth's figure axis, and then producing negligible variation of inertial moment.

Lomnitz and Nilden-Hofseth (2005) proposed that the tsunami may have been generated by in-phase action of the ${}_0S_2$ and ${}_0S_3$ spheroidal normal modes. Although ${}_0S_2$ and ${}_0S_3$ frequencies are present in the spectra of the tide-gauge records, the conclusions of the authors are not incompatible with a bulging of the sea floor and with the generation of the first tsunami wave by this bulge. Only a protrusion of material can explain both the normal mode excitation and the rotation pole displacement.

I submit that the discrepancy between surface wave M_o and normal mode M_o should be considered an important anomaly – in the Kuhn (1969) sense – whose clarification could lead to a substantial transformation of our view, recognizing the inadequacy of the pure elastic rebound model,

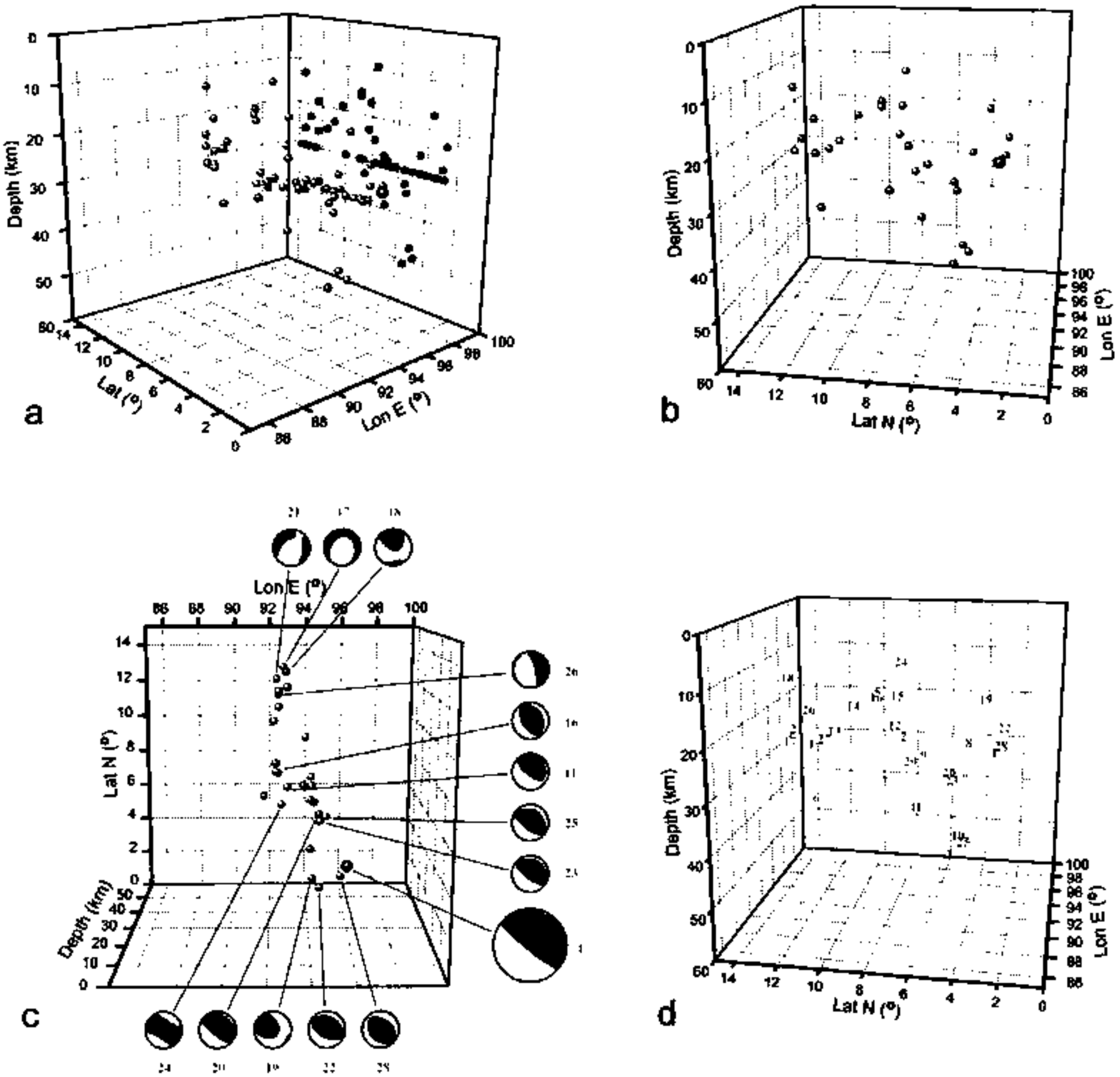

Fig. 9. a) The total number of events in the time window of two days (26 and 27 December) is 56 hypocentres (green and red spheres), which are also projected on the XZ plane as grey spheres. Green spheres are the seven events plotted in Figure 8. b) Residual distribution of 29 hypocenters is shown, after the elimination of the events with an assigned depth at 30 km. A small group of hypocenters having depth nearly 50 km is present near the event number 3. c) Observing vertically, no definite structure showing a NNE direction of subduction dipping can be seen. Focal mechanisms are also inconsistent with the subhorizontal subduction interpretation. The available Harvard CMT focal mechanisms are numbered following the event numbers in Figure 9d and Table 2. d) In order to facilitate the understanding of the spacetemporal hypocentral pattern, the progressive chronological numbers are shown for the 29 selected events.

and moreover, of the subduction hypothesis. Here I search for a solution by adopting the nearly vertical slip plane of the conjugate P2 fault solution instead of following plate tectonics prescriptions.

Indeed, assuming an average rigidity of $5.0 \cdot 10^{11}$ dyn/cm^2 (see Table A.3 in Bullen and Bolt, 1985), with 15 m of slip on a near-vertical fault 1200 km long and 50 km deep (the maximum depth of a brittle fracture) we obtain a moment

$$M_o = \mu \cdot s \cdot A = 5.0 \cdot 10^{11} \text{ dyn/cm}^2 \cdot 1.5 \cdot 10^3 \text{ cm} \cdot 1.2 \cdot 10^8 \text{ cm} \cdot 0.5 \cdot 10^7 \text{ cm} = 4.5 \cdot 10^{29},$$

which agrees with the M_o measured using long period surface waves. With the adoption of the P2 fault parameters, there

Table 3

The ten largest earthquakes since 1900

Location	Date	Magnitude (M_w)
1. Chile	May 22, 1960	9.5
2. Prince William Sound, Alaska	March 28, 1964	9.2
3. Andreanof Islands, Aleutian Islands	March 9, 1957	9.1
4. Kamchatka	Nov. 4, 1952	9.0
5. Off western coast of Sumatra, Indonesia	Dec. 26, 2004	9.0
6. Off the coast of Ecuador	Jan. 31, 1906	8.8
7. Rat Islands, Aleutian Islands	Feb. 4, 1965	8.7
8. Northern Sumatra, Indonesia	March 28, 2005	8.7
9. India-China border	Aug. 15, 1950	8.6
10. Kamchatka	Feb. 3, 1923	8.5

Source: National Earthquake Information Center, U.S. Geological Survey.

is no need to limit the slip zone to the southern third of the aftershock zone. The apparent excess seismic moment derived from the ${}_0S_2$ and ${}_0S_3$ modes (Stein and Okal, 2005) might be linked to a large amount of energy release, not by an 'elastic rebound' process but as a non-elastic displacement of materials – presumably a vertical flow – that has caused the strong ${}_0S_2$ and ${}_0S_3$ excitation, and the Earth's instantaneous rotational pole displacement. This vertical displacement should have bulged the belt zone between the Sunda Trench and the proposed rupture line (Figure 7, bold dotted line).

On the other hand, if the assumption of a sub-horizontal fault is adopted, using a single couple model (Julian *et al.* 1998; Miller *et al.*, 1998), we may account for the observed seismic moment but not for the displacement of the Earth's rotation axis. A near-vertical fault could agree with both the seismic moment and the polhody shift. Some scientists have attributed the observed displacement of the polhody to chance or to atmospheric forcing (Gambis, 2005; MacMillan, 2005), because the precise azimuthal relation between polhody displacement and epicentre position – shown in Figure 1 – has not been generally recognized by the geoscientists community.

An analogy can be envisaged between the mass movement that occurred during the Sumatra event and some typical volcanic earthquakes. The spectra of some volcanic earthquakes tend to be displaced toward the low frequencies. Most of these volcanic earthquakes cannot be described by a double couple (Julian *et al.*, 1998; Miller *et al.*, 1998). They are more destructive than might be expected from their low M_b value, as computed from 1 sec period waves. However, M_s as computed from lower frequencies, at 20-30 sec, provides a more realistic estimate of energy and damage. A possible origin of such volcanic events could involve laccolite or dike emplacement, or coseismic volcano flank gravitative sliding. Large earthquakes with an excess of low frequency energy can similarly be ascribed to slow phase changes involving expansion of a suitable volume of deep materials. To be more specific, one might suppose that these extremely large earthquakes might involve elastic rebound plus upwelling of mantle material constituting a substantial non-elastic additional portion of the mass movement.

SEA-LEVEL VARIATION AND SATELLITE DATA IN SUMATRA

Published preliminary results of the Geographic Survey Institute of Japan show post-seismic level variations of the coast over the entire region. Data are provided by satellites Radarsat-1, Envisat, ERS-1/2, Aster, Spot-5, updated to March 10, 2005. The coralline barrier to the west has been uplifted by the earthquake, and the Andaman Islands and parts of the north-west coast of Sumatra subsided (Searle, 2005). This is in agreement with the framework of this paper.

Bilham (2004) reports further geodetic results in good agreement with the postseismic level variation revealed by the satellites.

A new interpretation of emergence and submergence of coral micro-atolls (Sieh *et al.*, 1999; Zachariasen *et al.*, 1999; Zachariasen *et al.*, 2000; and others) suggests a possible cyclic uplift and subsidence of the coral rings. The authors propose the applicability of a plate tectonic model as in Figure 4. In this case, the atolls should slowly subside due to the push or pull of the subducting slab until the earthquake allows them jump back and rise. However, the evidence suggests a sudden subsidence in the geological past.

In Figure 7 the uplifted and subsided zones reported by the Japanese GSI are shown in red and in yellow, respectively. The proposed vertical rupture (bold dotted line) is the divide between the uplifted and subsided areas. Large ofiolite formations in the Nicobar and Andaman islands (Coleman, 1977) represent further evidence of a near-steady uplift of the arc in geologic time, and of a different rate of emergence along the Sunda Arc. The sudden subsidence might be explained as a part of the process of vertical fracture of the crust (Figure 6).

The GRACE satellites (Han *et al.*, 2006) observed variations of surface gravity of -15 μGal east of the Sunda trench, and a symmetrical anomaly of +15 μGal west of the trench. This pattern of anomalies does not fit a fault dislocation without a substantial lateral and vertical expansion of the oceanic crust to be added to the model. Han *et al.* (2006) adopt initially a subhorizontal slip in agreement with the focal mechanism, but the fit to the gravity data is poor. Their suggestion of local expansion supports the class of models proposed in this paper in Figure 6.

CASE-HISTORIES OF GREAT EARTHQUAKES. CHARACTERISTICS AND ANALOGIES

Common characteristics among large earthquakes of the past can help clarify the processes at the seismic source. The greatest moment magnitude (M_w) seismic events of the past century are listed in Table 3.

Event 8 is probably an aftershock of the earthquake of December 26, 2004. The more recent events are numbered 1, 2, and 7. The first two have been extensively studied by the scientific community.

Chile earthquake

A large seismic event struck the Chilean coast at 19.10:40 UT on May 22, 1960 (Plafker and Savage, 1970; Cifuentes, 1989; Cifuentes and Silver, 1989). The hypocenter was at 38.05°S – 72.34°W and the focal depth was estimated around 35 km, similar to the Sumatra earthquake. A recent relocation (Krawczyk and the SPOC Team, 2003) provides a more western and slightly deeper hypocenter > 73° 05' W, 38° 15' S, H = 38.5 km). This new hypocenter was based on 3D seismic imaging of the crust from the SPOC'experiment which shows the hypothetical subduction slab in a more westerly position. The relocation by more than 75 km may be considered a further anomaly from the point of view of the currently accepted geodynamic picture. The earlier epicentre is closer to the volcanic range.

The Chilean earthquake was preceded by a sequence of foreshocks that began 33 hours before the main shock (USGS, 2006). It ruptured 150 km of the northern segment of the fault. The records suggest that a large slow and silent foreshock took place on the deepest portion of the fault 15 minutes before the main shock, with a seismic moment comparable to that of the main event (Plafker and Savage, 1970; Kanamori and Cipar, 1974; Lund, 1982; Cifuentes, 1989; Cifuentes and Silver, 1989). Lund (1982) assumed that a solitary wave (soliton) was generated by this foreshock of 7.9 M_w. This precursor was detected on the strainmeter at Pasadena. It was modelled tentatively – using the observed surface deformation (Figure 10a) – by Linde and Silver (1989). The moderate uplift of the coastline was explained as a double slope fault that started to slip slowly at the deepest edge (Linde and Silver, 1989). In this case, the rupture would have to nucleate in the subcrustal ductile lithosphere where the stress produced by the subducting slab would dissipate. Barrientos and Ward (1990) propose a fault of variable slip to fit the surface displacements. The deeper portion of their displacement field was attributed to postseismic creep, but the precursor remains unaccounted for. The zero-slip line divides the two zones into more superficial and deeper slip, thus posing some severe mechanical problems.

Another problem is the amount of slip on the alleged 20° dipping fault. A computed slip of nearly 20 m is at odds with the Nazca-South America convergence rate of nearly 8 cm/yr, as it suggests 250 years of earlier strain accumulation. This problem is also found among other great earthquakes.

The association of volcanic phenomena with strong earthquakes was documented by Charles Darwin (1809-1882) in the 1835 Concepcion earthquake (Darwin, 1897, page 236):

"I have [in other papers] given an account of the remarkable volcanic phenomena, which accompanied this earthquake. These phenomena appear to me to prove that the action, by which large tracts of land are uplifted, and by which volcanic eruptions are produced, is in every respect identical".

And in the more detailed description (Darwin, 1840):

"*We see, therefore, that, in 1835, –the earthquake of Chiloe, –the activity of the train of the neighbouring volcanoes, – the elevation of the land around Conception, –and the submarine eruption at Juan Fernandez, took place simultaneously, and were parts of one and the same great phenomenon.*"

In the 1960 Chile earthquake, 17 of 38 active Andean volcanoes (Casertano, 1963) had eruptions or other minor volcanic activities within a few months of the earthquake. The following erupted in close coincidence with the seismic event: Copahue, Llaima, Villarrica, Cordon, Calbuco, Lautaro. There were also eruptions of volcanoes to the north: Planchon-Peteroa, San José, Tupungatito, Lascar, San Pedro, Guallatiri (Casertano, 1963; Smithsonian Institution, 2006).

Similar correlations occurred along all the Cordillera on the occasion of the 1906 Ecuador earthquake (Mw=8.8), including eruptions of Puracé and Reventador in the north, Ubinas in the central section and Cerro Azul, Nevados, Villarrica, Calbuco, Huequi in the South (Smithsonian Institution, 2006). The history of correlation between earthquake and volcanic phenomena on the South American Cordillera can be traced back in the time, finding descriptions of them also in seventeenth century European books (d'Avity, 1643; Placet, 1666, see pages 74-78 of first edition).

In Figure 11 the data from the Smithsonian catalogue are shown for South American eruptions from 1800 to 1999. There are some interesting peaks which coincide with major earthquakes. Whether the correlation is real or coincidental is still a matter of debate. However, the data suggest a possible link between Wadati-Benioff earthquakes and volcanic phenomena, due to a rise of deep material (Scalera 1997, 2006b, 2006c).

Except for transform fault earthquakes and shallow tectonics events, all problems and paradoxes may thus be resolved in a more natural way. A sudden aseismic change of phase can produce an increase of volume at great depth – in a tensional regime – with elastic fracture of the overlying brittle material and continued anelastic flow.

Alaska earthquake

In the late afternoon of March 27, 1964, the second largest earthquake (but eventually the largest on recent reassessment of magnitude by Okal – seminar at INGV headquarters) ever experienced by mankind struck the gulf of Alaska, with epicentre (61.0°N, 147.7°W) about 150 km east of Anchorage, near College Fiord (Anonymous, 1964). In the map attached to the first available report (Anonymous, 1964) a delineation of the uplifted and subsided zones is drawn (Figure 10b).

As in the Sumatra earthquake, in the Alaska seismic event a long belt – at least 500 km – of subsided crust followed an inner zone from near Anchorage to Kenai Peninsula and Kodiak Island. A subsidence of up to 2.0 m was recorded. An emergence zone with a peak uplift of 8 m was recognized on the external region facing the Pacific. It was probably of the same length as the subsided one. The absence of islands far from Prince William Sound made impossible a precise estimate of the uplifted belt length (Anonymous, 1964; Landen, 1964; Plafker, 1965). The focal mechanism of the event was determined by various authors (Press and Jackson, 1964; Savage and Hastie, 1966; Stauder and Bollinger, 1966) and a discussion developed about the true slip surface, i.e. the main or conjugate fault solution. The hypothesis of a sub-horizontal thrust fault was favoured from comparison between observations of vertical displacements and modelled ones (Plafker, 1965; Savage and Hastie, 1966; Stauder and Bollinger, 1966).

The early focal mechanism determination by Press and Jackson (1964) was definitely a vertical blind fault of 200 x 800 km at 15-20 km depth. However, Plafker (1965) suggested the possibility of both main and conjugate fault solutions. Savage and Hastie (1966) and Stauder and Bollinger (1966) followed Plafker's suggestion of a sub-horizontal rupture but remained undecided between the two alternative fault-plane solutions. Shortly after, the advent of plate tectonics was decisive in the steering of the choices of the geosciences community, but the question is still open.

As Charles Darwin noted (1897) for South America, the movement of uplift and subsidence of the coastlines is very complicated, and sometime linked with volcanic and seismic events. My idea is that these vertical movements are the result of deep anelastic displacements of visco-plastic material, which can precede, go along, as well as follow, the elastic fracture. These displacements can interact in a complicated way with the inhomogeneities of the crustal cover, producing an irregular pattern superimposed on a more extended regular trend (i.e. the elongated trends of subsidence and emergence in the great earthquakes of arcs).

Chi-Chi, Taiwan, earthquake

On September 21 1999, a magnitude Mw=7.6 earthquake (not listed in Table 1) occurred near the town of Chi-Chi, Taiwan (23.85°N, 120.81°E), causing more than 2400 dead. The earthquake was a 'subduction-related' crustal event (depth=7.0-10.0 km) (Abrahamson *et al.*, 1999; Shin *et al.*, 1999; Cattin *et al.*, 2004). It ruptured 85 km of the N-S Chelungpu Thrust Fault. According to the current interpretation, Taiwan is a result of collision between the Eurasian continent and an island arc. The Eurasian plate is envisaged as subducting towards east, under the Luzon arc.

The interpretation was judged problematic because, albeit a subduction event, the surface deformation (Lin *et al.*, 2001; Johnson and Segall, 2004) was steeper than the expected sub-horizontal fault in the initial superficial segment of a subducting slab (Seno, 2000; Seno *et al.*, 2000). A propagation of the rupture was hypothesized along a sub-horizontal decollement, but the western edge of the fault became progressively steeper up to its final surface vertical emersion.

Some difficulties arise of the hypocenter distribution of the aftershock sequence (Kao and Chen, 2000; Johnson and Segall, 2004). It is uneven and presents at least three groups of hypocenters at different locations and depths. A group (labelled B10, B12, B24, B25 in Kao and Chen, 2000) is nearly 50 km east from the main shock, on the eastern side of the orogen. This group may correspond to a wide and

complex mass-movement involving the entire orogen. The deeper group of aftershocks (depth 25-37 km) bears witness to the plutonic origin of the mass movement.

While in the western side of the orogen the Pliocene and Miocene strata (1.8-23.8 Ma) are correctly located, the Oligocene facies (23.8-33.7 Ma) are unconformally superimposed on the younger ones (Figure 1c in Johnson and Segall, 2004). The Oligocene represents the more central axes of the Taiwan orogen and this inverted age pattern of the geologic facies is typical of a pronounced uplift of the orogen core followed or accompanied by a lateral spreading and thrusting on the younger low-land (Ollier, 2002, 2003; Ollier and Pain, 2000).

Similar phenomena of lateral spreading are well documented by geologic and geodetic surveys on young orogens (Coltorti and Ollier, 2000; Ollier, 2002, 2003; Ollier and Pain, 2000; Saroli *et al.*, 2005; Serpelloni *et al.* 2006).

This is a further case of vague or unfavourable evidence of sub-horizontal underthrust, and many efforts are actually dedicated in Taiwan to made more clear both the geological setting of the region and the fault geometry (by deep drilling).

The historical Calabrian earthquake sequence of 1783

On 5 February 1783 a seismic sequence occurred in Calabria, southern Italy, along the superficial part of the Sicilian-Calabrian arc and the Wadati-Benioff zone. The main shocks of the sequence occurred in two months and the data were (*INGV-Catalogue of the Strong Italian Earthquakes*, Boschi *et al.*, 2000: http://storing.ingv.it/cfti/):

5 Feb. (lat. 38.30 - lon. 15.97) XI degree MCS,
6 Feb. (lat. 38.22 - lon. 15.63) VIII-IX MCS,
7 Feb. (lat. 38.58 - lon. 16.20) X-XI MCS,
1 Mar. (lat. 38.77 - lon. 16.30) IX MCS,
28 Mar. (lat. 38.78 - lon. 16.47) XI MCS.
(latitude and longitude are in degrees and cents of degrees)

The five epicentres – which was determined by macroseismic effects and isoseismal maps – occurred progressively more N-NE on an elongated path of nearly 100 km length (Tiberti *et al.*, 2006). The cumulative effects of this five main shocks of the sequence and of their three years long series of aftershocks produced damages so impressive and wide that would deserve to be classified by the statements which define the XII MCS degree (*Total damage - Almost everything is destroyed. Lines of sight and level distorted. Objects thrown into the air. The ground moves in waves or ripples. Large amounts of rock may move*).

Indeed, typical in this seismic event was the sliding of whole hills towards the valley floors, in some cases dragging complete towns for hundreds of meters. Many rivers were obstructed and lakes were created. On the Tyrrhenian site, near Scilla, a huge landslide with a front of near 3 km made a portion of Mount Campallà falled and disappeared in the sea (Tiberti *et al.*, 2006). I cite this sequence as example of slow propagation of stress along an arc, of documented sparse punctuated episodes of surface masses sliding triggered by earthquakes – which contribute to the spreading of an orogen in geological time –, and of all these occurrence of phenomena just on an orogen in a documented present state of uplifting (e.g. see Calabrian coastal terrace analysis in Valensise and Pantosti, 1992; Cucci, 2004; Cucci and Tertulliani, 2006). Further possibly coseismic uplift occurred during the Calabrian earthquake of 1905 (Sept. 8, lat. 38.67, lon. 16.07, I_o=X MCS), as documented by terraces creation along Calabrian Tyrrhenian coasts (Cucci and Tertulliani, 2006). Hypothesis on possible vertical slip along vertical faults has been made by Galli and Bosi (2003) reanalysing the catastrophic 1638 Calabrian earthquake. Again I see – this time in the Recent – the action of the earthquakes in contributing – as part of a long causal chain – to the mountain building and spreading, as already highlighted analysis of mine (Scalera, 1997, 1006c, 2007) and of others (Moretti and Guerra, 1997) and in satellite imaging results (Saroli *et al.*, 2005).

Transform fault earthquakes

All the preceding considerations are about contradictions on the subject of Wadati-Benioff zone earthquakes, as revealed by near-surface 'subduction' earthquakes. But as concerns strike-slip earthquakes in transform zones, comparable problems exist. The Parkfield experiment in California was set up with the aim to confirm the recurrence of strong earthquakes in the Parkfield segment of the San Andreas fault (in 1857, 1881, 1901, 1922, 1934, 1966) and the mechanical model of earthquake occurrence, proposed by Reid in 1906. According to this model, an earthquake occurs when an increasing stress overcomes the frictional static stress of a pre-existing fracture, or the strength of the brittle material. The event did not occur before 1993, as forecasted, and the geophysical arrays of strainmeters and other instruments did not recorded a significant accumulation of strain or other geophysical precursors around 1993 nor before 2004, when the event at last happened (Lindh, 2005; Langbein *et al.*, 2005). Certainly this result, if confirmed, is a refutation of the alleged mechanism of stress-strain accumulation currently accepted by global tectonics.

WADATI-BENIOFF ZONES

In this section a brief review of a number of 'subduction' zones at active margins will be made. Some common characteristics are highlighted, and the incompatibility of these peculiarities with plate tectonics is stressed (Scalera, 2006b, 2006c). The new features of the Wadati-Benioff

zones are made visible (Figure 12abcdef) using the relocated hypocentral data by Engdahl *et al.* (1998).

Mediterranean

The Mediterranean is characterised by two well-defined regions of deep earthquakes (Berckhemer and Hsü, 1982; Cadet and Funiciello, 2004; Scalera, 2004, 2005c; Vannucci *et al.*, 2004). The focal depth does not exceed 200 km in the Aegean region, while it reaches more than 400 km in the southern Tyrrhenian region (Figure 12a). Minor spots of intermediate depth earthquakes are present under the northern Apennines (depth up to 60 km), around the Gibraltar region (two non relocated hypocenter show a depth greater than 500 km, while are absent in the Engdahl *et al.*, 1998, catalogue) and under the narrow, tube-like, near-vertical focal volume in Vrancea, Romania (depths 60-200 km). There is an opinion that the cause of deep seismicity is a subductive process, but there is some doubt in the case of Vrancea, currently interpreted as a relic of a former wide Carpatian Wadati-Benioff zone.

Careful reconstructions of Pangea (Bullard *et al.*, 1965; Owen, 1983; other references in Scalera and Jacob, 2003) suggest little deformation of plates in geologic time. Thus a non-uniform pattern of deep hypocenters is unlikely to be generated by Africa-Eurasia interaction by a uniform motion of two plates. Moreover, in this region the consistent amount of evidence of extensional processes is at odds with the alleged Africa-Europe convergence (Michard, 2006; among others). Especially impressive in Figure 12a, and at odd with plate tectonics is the presence of narrow pipe-like distribution of hypocenter under Vrancea and South Tyrrhenian region, which both are located under zones of maximum curvature of the relative arcs (Calabrian arc and southern 'syntaxial' zone of Carpatian arc). Similar situation is valid for Indian Himalayan arc (see next section). New interpretations in a framework of a progressively enlarging Tethys and Mediterranean region are needed (Scalera, 2005b).

India

The India-Asia collision generates deep hypocenters only under the two syntaxial zones of the Himalaya (Figure 12b). Due to the small extension of the India fragment, the same or greater reservations may be raised as in the case of the Africa-Europe collision. The expected distribution of deep foci should be more uniform and the two syntaxial zones should be connected by a well developed Wadati-Benioff zone. But in addition to the absence of deep foci, a slope that is opposite to the expected is found under the western deep foci zone, and here some filaments of hypocentres are discernible (Figure 12b).

Most Himalayan crustal seismicity (depth range 0-40 km, not plotted in Figure 12b) has compressional focal mechanisms on the Indian margin and tensional ones on the Tibet one. This agrees with an orogen in a gravitational spreading phase, without need to made recourse to continental collision. Moreover the Himalaya is caracterized by a clear zone of extrusion of deep material – verging toward south – in clear contradiction with the alleged subductive process (Beaumont *et al.*, 2001; Hodges *et al.* 2001; Ernst, 2005; among others). A confutation that this extrusion is totally due to the combined action of atmospheric erosion and isostasy has been proposed by Ollier (2006b). The documented extrusion front of Himalaya fits with the general meaning of this paper and is probably linked to plutonic phenomena leading to material expansion and uprising.

Sunda

In its segment from Sumatra to the Andaman islands, the Sunda arc has hypocenters not deeper than 250-300 km. Deepest seismicity is present under Java up to New Guinea, with focal depths up to 700 km. Here the hypocenters have the tendency to cluster in large columnar zones of which the great islands and groups of islands are like (architectonic) capitals (Figure 12c). The alleged uniform northward motion of the Indian plate sea-floor under Sunda arc (Puspito and Shimazaki, 1995; Hafkenscheid *et al.*, 2001) – besides a near tangential motion on the Andaman arc segment, which poses severe mechanical problems – should produce a similar uniform downgoing motion of the subducted slab, without preferences of earthquakes to occur under the islands. Many evidences of prevailing extensional and vertical tectonics regimes has been collected by Lindley (2006) on the New Guinea boundary between the Australian and Pacific plates, that are ad odds with the current alleged convergent movements of the two plates. Then 'subduction' is unlikely as source of this the non-uniform columnar-filamentous hypocentral pattern observed under that boundary.

East Asia arcs

Most classical iconography of the Wadati-Benioff zone in the 'subduction regions' is taken from narrow vertical sections perpendicular to the East Asia arcs (Figure 13a). The quite good alignment of hypocenters along a slope dipping ≈45° in the Honshu region (Figure 13a) is part of a set of possible cases (smaller slope, higher slope, curved, two slope, broken, etc.) described in the current theory for a number of different Wadati-Benioff regions, but ever in a two-dimensional representation.

If observed in a different way – and taking advantage of the recently available higher quality relocated hypocentral data (Engdahl *et al.*, 1998) – the reality appears somewhat more complicated. Plotting all East Asian Wadati-Benioff zones in 3D, using a larger scale, from Kamchatka Peninsula to the China Sea and the Marianas, the irregular and filamentous structure of the subduction zones is highlighted

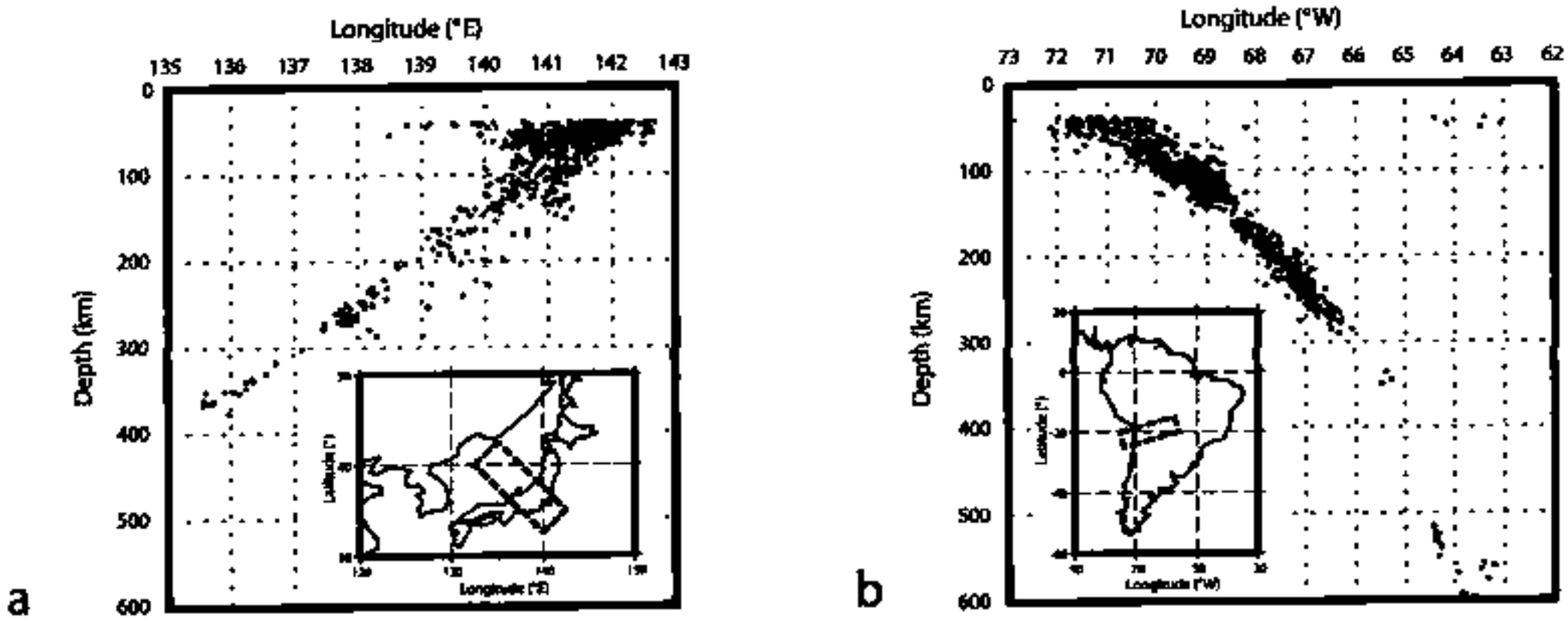

Fig. 13. Two examples of classical two-dimensional representation of Wadati-Benioff zones, with hypocentral depth greater or equal to 40 km. a) A section-box under the Japanese arc. b) A section under the central part of the South American Cordillera.

(Figure 12d). No direct link between this kind of uneven pattern and the subductive process can be easily invoked. Also the alleged spoon-like structure of the Wadati-Benioff zone is not clearly recognizable. Considering that the alleged displacement of the Pacific plate follows the WNW direction of the Hawaii islands chain, and that the major fracture zones in the Jurassic seafloor of Western Pacific aligns near parallel to the Asian arcs, also in this case a near uniform rate of subduction should be expected and a consequent greather uniformity of the deep hypocentral distribution.

South America

Classical two-dimensional plottings of vertical sections the hypocenters under the Central Andes mountain belt (see an example in Figure 13b) show a regular dipping pattern of hypocenters up to 300 km depth, with a tendency towards a lower slope in the lithosphere (0-100 km, Figure 13b) and a long zone of absence of seismic foci between 350 km and 500 km. Instead, in the three-dimensional views shown in Figure 12ef, all the South American Wadati-Benioff zone – from Colombia to Cape Horn – is characterised by strong inhomogeneities in the hypocentral spatial distribution, with focal zones tapering toward deep points.

In Figure 12ef, the vertical scale has been greatly enhanced to highlight the unexpected pattern of these seismofocal zones. The brown circles represent the seventy-two volcanoes along the Andes Cordillera, which has been active in historical time (data from Smithsonian Institution, 2006). The volcanic provinces are grossly divided in relation to the seismofocal zone features. Some North-South gaps in the deep hypocentral pattern are in relation to gaps and lower density of the volcanoes distribution, adding further elements to the possible stronger-than-supposed link between seismic and volcanic phenomena (Scalera, 1997). Geomorphic and tectonic field studies of the Andes points toward a rapid uplift of the Cordillera from Miocene, and the creation of the Interandean Depression as result of a lateral spreading (Coltorti and Ollier, 2000), which is at odd with a compressional origin of the orogen. Very problematic, in a region in which subduction is credited to be in a steady-state activity at least from Cretaceous, is the young age of the uplifting and the tectonic stand-still that allowed a recognized planation phase of the Cordillera (Coltorti and Ollier, 2000). A different font of energy for mountain building should then be searched for, in agreement with the requirements of this paper.

In conclusion of this brief and incomplete review: using a more general, wider scale, ad three-dimensional view, together with higher quality data (Engdahl *et al.*, 1998), it is possible to recognize that Wadati-Benioff zones do not correspond to what is prescribed by plate tectonic theory, and to what we expect to see having in mind the narrow hypocenters vertical sections of the classical seismological iconography (e.g. Figure 13ab). Filaments of hypocentres characterize the large scale 3-D plots of the catalogue of the relocated events (Figure 12abcdef). These filaments are real characteristics of hypocenter distribution because their separation can easily reach an order of magnitude of degrees. The filaments have the tendency to taper in depth, leading to the idea of a narrow origin of the disturbance, which propagates and becomes progressively wider toward the surface. Instead of a downgoing subduction they evoke the image of trees, or smoke coming out of chimneys.